

Intelligent Reflecting Surface Aided Multiple Access Over Fading Channels

Yiyu Guo, Zhijin Qin, *Member, IEEE*, Yuanwei Liu, *Senior Member, IEEE*, and Naofal Al-Dhahir, *Fellow, IEEE*,

Abstract

This paper considers a two-user downlink transmission in intelligent reflecting surface (IRS) aided network over fading channels. Particularly, non-orthogonal multiple access (NOMA) and two orthogonal multiple access (OMA) schemes, namely, time division multiple access (TDMA) and frequency division multiple access (FDMA), are studied. The objective is to maximize the system average sum rate for the delay-tolerant transmission. We propose two adjustment schemes, namely, dynamic phase adjustment and one-time phase adjustment. The power budget, minimum average data rate, and discrete unit modulus reflection coefficient are considered as constrains. To solve the problem, two phase shifters adjustment algorithms with low complexity are proposed to obtain near optimal solutions. With given phase shifters and satisfaction of time-sharing condition, the optimal resource allocations are obtained using the Lagrangian dual decomposition. The numerical results reveal that: i) the average sum rate of proposed NOMA network aided by IRS outperforms the conventional NOMA network over fading channels; ii) with continuous IRS adjustment in the fading block, the proposed TDMA scheme performs better than the FDMA scheme; iii) increasing the minimum average user rate requirement has less impact on the proposed IRS-NOMA system than on the IRS-OMA system.

Index Terms

fading channels, intelligent reflecting surface, non-orthogonal multiple access, resource allocation.

Y. Guo, Z. Qin and Y. Liu are with School of Electronic Engineering and Computer Science, Queen Mary University of London, London E1 4NS, U.K. (e-mail: yiyu.guo@qmul.ac.uk; z.qin@qmul.ac.uk; yuanwei.liu@qmul.ac.uk).

N. Al-Dhahir is with the Department of Electrical and Engineering, The University of Texas at Dallas, Richardson, TX 75080 USA (e-mail: aldhahir@utdallas.edu).

I. INTRODUCTION

Higher demands on spectrum efficiency, energy consumption, and massive connectivity have been placed for the fifth generation (5G) and beyond wireless communication systems [1–3]. Intelligent reflecting surface (IRS) technology has gained extensive attention recently. Specifically, IRS is a metasurface consisted of multiple passive reflecting elements, which enables dynamic change the signals direction [4, 5]. Its ability of controlling the signals reflection and adjusting the propagation environment can lead to performance gain with low power costs [6].

IRS-assisted communication shares the similarity with the amplifying and forwarding (AF) relay communication and backscatter communication, but also with some important difference [7–9]. The AF relay requires active signal processing and retransmits the amplified signal. While IRS elements only reflect signals passively without introducing any active processing of them [10, 11]. Hence, IRS can greatly reduce energy consumption [12]. This feature also enables the IRS to work in full-duplex mode, which can avoid the self-interference in comparison with the full-duplex AF relay [13]. For the backscatter communication, either a dedicated source or ambient source is needed for backscatter communication [14–17]. Backscatter devices transmit its own information and modulate the incident signal while the IRS provides an additional link without introducing its own information [18].

To fully achieve the passive beamforming gains of IRS, multiple access techniques are of significant importance [19]. Based on design principles, multiple access schemes can be classified as orthogonal multiple access (OMA) and non-orthogonal multiple access (NOMA) [20]. Conventional OMA communication orthogonally serves one user in a single time/frequency/code domains or combinations thereof resource block [21]. By contrast, the successive interference cancellation (SIC) technique enables the power domain NOMA scheme to achieve a higher number of connections in one resource block [22]. The features of NOMA scheme has been widely studied recently [23–25].

A. Related Works

The study and design of IRS-assisted networks have focused towards new challenges of IRS passive beamforming [26, 27]. Various wireless communication networks assisted by the IRS have been investigated for verifying its performance gain [28]. An IRS aided multiuser multiple-input single-output (MISO) system was investigated for the single cell case in [29]. By optimizing

reflection coefficients of IRS elements, the power consumption can be significantly reduced. IRS was utilized for secure transmission relying on cooperative jamming techniques in [30, 31]. The system fairness was considered in [32], neglecting the direct link for blockage, and the users' minimum rate was maximized with IRS assisted. The IRS has also been used to enhance the rate performance in [33].

Beside the works aforementioned under the OMA schemes, recently, some researchers have investigated the efficient integration of IRS with NOMA to enhance spectrum and energy efficiencies. [34, 35]. A SISO-NOMA IRS-assisted network was proposed in [36], where a prioritized design was proposed for further enhancing spectrum and energy efficiencies. To solve the beamforming and IRS design problems, a difference-of-convex (DC) algorithm was applied in [37]. By considering the target data rate constrain, decoding order problem was also investigated. The decoding order problem was also studied in [33] and users were ordered base on the combined channel gain. The authors in [38] proposed a 1-bit coding scheme on the IRS, which transmits signals to the NOMA users as a relay. With the ability of adjusting the signal directions, the IRS has been regarded as a promising technology that illustrates important advances with the implement in NOMA networks [39].

Moreover, dynamic resource allocation over fading channels significantly enhances the performance compared with fixed resource allocation in static channels [40]. In systems with fading broadcast channels, power, time and bandwidth are adaptively assigned among users based on the channel state information (CSI). Particularly, the dynamic resource assignment policies under various multiple access schemes were proposed in [41] and [42], which assumes that perfect CSI are obtainable from the transmitter and receivers. The corresponding ergodic capacity region and the outage capacity region were studied as well. By utilizing spectrum sensing and sharing, an power assignment policy was investigated in [43] for maximizing the achievable capacity under fading channels.

B. Motivations and Contributions

The most works on IRS-assisted systems were considered in static channels, which motivates us to develop a long term resource allocation policy for the IRS-assisted downlink networks over fading channels. Both OMA and NOMA schemes are investigated for comparison. Two types of OMA schemes, namely, frequency division multiple access (FDMA) and time division multiple

access(TDMA), are considered. To our best knowledge, such a dynamic optimization problem with multiple access schemes over fading channels scenario is still lack of studies. The main challenges of the considered system are identified as the following:

- The formulated resource allocation problem is non-trivial to solve as the objective functions is NP-hard.
- The globally optimal solutions is hard to obtain by efficient methods or algorithms, as the discrete unit-modulus constraints and the non-convexity lie in the optimization problems.
- The long term design is expected for the coupled IRS adjustment and resource allocation problems over fading channels.

In sight of the above challenges, we consider the joint phase shifters policy and resource assignment optimization problems in downlink IRS-assisted systems. The major contributions are outlined below:

- 1) A downlink IRS-aided system over fading channels is considered, where two users are served by different multiple access techniques, namely, NOMA, TDMA and FDMA. We propose two IRS adjustment schemes based on the timing of altering reflection coefficients. A joint phase shift and resource allocation problems are solved for the average sum rate maximization problem.
- 2) For the IRS design, we apply the success convex approximation (SCA) to solve the IRS adjustment problems, where the sequential rank-one constraint relaxation (SROCR) method is applied for the rank-one constrain for NOMA and OMA. Low complexity algorithms are proposed for IRS phase adjustment.
- 3) For the resource allocation, we utilize the Lagrange duality method for the non-convex problems. The formulated average sum rate maximization problems for all multiple access schemes meet the time-sharing condition, then adaptive solutions that achieve maximum data rate over fading channels are obtained.
- 4) Alternating optimization (AO) algorithms are proposed to optimize IRS reflection coefficients and power allocation efficiently. The proposed communication networks can enhance the system effectiveness by integrating IRS and NOMA. Numerical results demonstrate the utility of the proposed methods.

C. Organization and Notations

The remainder of this paper is organized as follows. In Section II, the system model is presented. In Section III, two IRS adjustment policies and phase shifters optimization problems are formulated first. Then the proposed design to solve the resource allocation problem for the IRS-aided network is presented in detail. We then provide the simulation results to verify the theoretical analyses in Section IV. The conclusions follows in Section V.

The main notations used are shown as follows. $\mathbb{C}^{N \times 1}$ denotes the space of $N \times 1$ complex-valued matrices and $\text{diag}(x)$ denotes a diagonal matrix whose diagonal elements are the corresponding elements in vector x . x^H denotes the conjugate transpose of vector x . The notations $\text{Tr}(X)$ and $\text{rank}(X)$ denote the trace and rank of matrix X , respectively. $\mathcal{R}e(x)$ and $\mathcal{I}m(x)$ denote the real and imaginary part of the complex number x , respectively. $[x]_a^b$ denotes the value of $\max(\min(x, b), a)$, and $\arg()$ denoting the component-wise phase of a complex vector.

II. SYSTEM MODEL

As shown in Fig.1, the considered downlink system consists of one base station (BS) with the single antenna, IRS with N passive reflecting elements and two users equipped with the single antenna, denoted by U_k , $k \in \{1, 2\}$. All channels are assumed that consist of large scale and small scale fading. The channel between BS and user k is denoted as h_k . The small scale fading between BS and user k is modeled as Rayleigh fading, then the corresponding channel can be expressed as

$$h_k = \sqrt{L(d)} f^{\text{NLoS}}, \quad (1)$$

where f^{NLoS} is the Rayleigh fading. The large scale pass loss is modeled as $L(d) = \rho_0 \left(\frac{d}{d_0}\right)^{-\varphi}$, where $\rho_0 = -30 \text{dB}$, and φ denotes the path loss exponent.

For the channel between BS and IRS and that between IRS and users, line of sight (LoS) components exist. Therefore, the small scale fadings effects in these channels are modeled as Rician fading. The channels from BS to IRS and IRS to users are denoted as $g \in \mathbb{C}^{N \times 1}$ and $r_k \in \mathbb{C}^{N \times 1}$, respectively. The resulting BS to IRS channel is following:

$$g = \sqrt{L(d)} \left(\sqrt{\frac{v}{1+v}} f^{\text{LoS}} + \sqrt{\frac{1}{1+v}} f^{\text{NLoS}} \right), \quad (2)$$

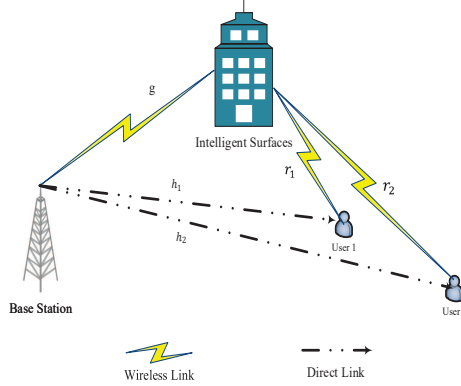


Fig. 1: Illustration of an IRS-assisted downlink NOMA network.

where v is Rician factor and f^{LoS} refers to the LoS component. The IRS to users channels are modeled in the similar way.

We assume that the complex channel coefficients $h_k(i)$, $G(i)$, and $r_k(i)$ experience block fading with a continuous joint probability density function (pdf), where i represents a fading state. Define $\Theta = \text{diag}(u) \in \mathbb{C}^{N \times N}$ as the IRS diagonal reflection coefficients matrix with $u = [u_1, u_2, \dots, u_N]$ and $u_n = \beta_n e^{j\theta_n}$, where $\beta_n \in [0, 1]$ and $\theta_n \in [0, 2\pi)$ refer to the amplitude of the reflection coefficient and phase shift of the n th IRS element, respectively.

Two multiple access schemes are considered, namely, NOMA and OMA. For the NOMA scheme, the two users share the same resource block simultaneously. For the OMA scheme, continuous time/frequency allocations are considered.

1) NOMA: A power-domain downlink NOMA scheme is implemented in the considered system. The signal transmitted to user 1 is given by

$$y_1(i) = (h_1(i) + r_1^H(i)\Theta g(i))(\sqrt{p_1(i)}s_1 + \sqrt{p_2(i)}s_2) + n_1, \quad (3)$$

where s_1 is the transmit signal intended for user 1 and $\mathbb{E}\{s_1^2\} = 1$; $p_1(i)$ denotes the transmit power for user 1; $n_1 \sim \mathcal{CN}(0, \sigma^2)$ is the additive white Gaussian noise (AWGN) with zero mean and variance σ^2 .

According to the NOMA decoding principle, the user with poor channel gain is assigned with a higher power budget and that with better channel condition performs SIC to remove the signal of the other user. Proper decoding order based on the channel conditions and transmit power

level can significantly enhance the NOMA transmission performance. While in IRS-aided NOMA networks, the combined channel gain is determined by both the direct link and the auxiliary IRS link, $h_k(i)$, $r_k^H(i)$ and $g(i)$. As Θ can be manually controlled, IRS significantly complicates user decoding order in NOMA scheme. With two users served in the system, we will consider all possible SIC decoding orders, denoted as Π .

Then, the signal-to-interference-plus-noise ratio (SINR) for user 1 at fading state i can be given by

$$\tau_1^{\text{NOMA}}(i) = \begin{cases} \frac{|h_1(i) + r_1^H(i)\Theta g(i)|^2 p_1(i)}{|h_1(i) + r_1^H(i)\Theta g(i)|^2 p_2(i) + \sigma^2}, & \text{if } \Omega(1)(i) = 1, \\ \frac{|h_1(i) + r_1^H(i)\Theta g(i)|^2 p_1(i)}{\sigma^2}, & \text{otherwise,} \end{cases} \quad (4)$$

where $\Omega(k)$ denotes the user k 's ordering and $\Omega(k) = 1$ means that user k 's signal will be decoded first. Then, the instantaneous achievable rate for user 1 is given by $R_1(i) = \log_2(1 + \tau_1^{\text{NOMA}}(i))$.

2) OMA: For the OMA scheme, the BS serves users in orthogonal frequency bands and time slots under FDMA and TDMA schemes, respectively. At the fading state i , the instantaneous achievable rate for user k is given by

$$R_k^{\text{OMA}}(i) = \alpha_k(i) \log_2 \left(1 + \frac{|h_k(i) + r_k^H(i)\Theta G(i)|^2 p_k(i)}{\alpha_k(i) \sigma^2} \right), \quad (5)$$

where $\alpha_k(i)$ denotes a fraction of the orthogonal resource at the fading state i , and $\alpha_1(i) + \alpha_2(i) = 1$ with $\alpha_k(i) \in [0, 1]$. The total power consumption in the FDMA scheme is same as that in the TDMA scheme, i.e., $\alpha_1(i) \frac{p_1(i)}{\alpha_1(i)} + \alpha_2(i) \frac{p_2(i)}{\alpha_2(i)} = p_1(i) + p_2(i), \forall i$.

III. JOINT PHASE SHIFT DESIGN AND POWER ALLOCATION

A. Problem Formulation

We consider the transmissions in delay-tolerant networks, which is tolerant with the propagation delay. Thus the number of codewords can be designed for a length that goes to infinity in theory. The users decode their desired signals from the BS in the entire fading procedure. Then, the users average sum rate are given by $\mathbb{E}_i[R_1^{\text{NOMA}}(i) + R_2^{\text{NOMA}}(i)]$ and $\mathbb{E}_i[R_1^{\text{OMA}}(i) + R_2^{\text{OMA}}(i)]$ for the NOMA scheme and OMA scheme, respectively.

Each fading state lasts a very short time, which makes it costly to adjust the intelligent surfaces continuously. Therefore, we consider two schemes for adjusting the phase shift.

- **Dynamic phase adjustment:** In this scenario, the IRS adjustment can be performed in every fading state based on the instantaneous transmit power for each user and channel state information obtained from the previous fading state. The transmit power, time and frequency allocation will be performed under given phase shifts.
- **One-time phase adjustment:** In this scenario, we divide all fading states into several blocks. The reflecting elements are adjusted at the beginning of each fading block based on the average transmit power for each user and CSI obtained from the previous block. The IRS in TDMA scheme will be optimised in the time slot same as that in the FDMA scheme for this scenario.

Remark 1. *There is a major difference between the FDMA and TDMA schemes under dynamic phase adjustment, namely that the IRS can be adjusted for a single user in TDMA transmission at different time slots while it needs to be optimised for both users to maximise the ergodic sum-rate in FDMA transmission.*

In delay-tolerant networks, the user with better channel condition is allocated with most resource budget for maximising the average sum-rate over the entire fading process, which motivates the designer to set a target rate for the poor user. Aiming at data rate maximization while guaranteeing the user fairness, we propose to jointly optimize the phase shift and resources allocation at each fading state or fading block. The optimization problem with the NOMA scheme can be formulated as

$$(\mathbf{P1}) \quad \max_{p_1(i), p_2(i), \Theta} \quad \mathbb{E}_i[R_1^{\text{NOMA}}(i) + R_2^{\text{NOMA}}(i)] \quad (6a)$$

$$\text{s.t.} \quad \mathbb{E}_i[p_1(i) + p_2(i)] \leq \bar{P}, \quad (6b)$$

$$p_1(i) + p_2(i) \leq \hat{P}, \forall i, \quad (6c)$$

$$p_1(i) \geq 0, p_2(i) \geq 0, \forall i, \quad (6d)$$

$$\mathbb{E}_i[R_k(i)] \geq \bar{R}, \forall k, \quad (6e)$$

$$0 \leq \theta_n \leq 2\pi, \forall n, \quad (6f)$$

$$\Omega \in \Pi, \quad (6g)$$

where \bar{P} denotes the average power budget that is determined by the total transmit power over the long term. \hat{P} denotes the peak power constraint determined by the transmit power budget at the fading state i . (6b) describes the average transmit power budget during the entire transmission procedure. (6c) limits the instantaneous total transmit power at one fading state. We can see that $\bar{P} \leq \hat{P}$. Constraint (6e) limits the minimum transmission rate for each user. Constraint (6f) limits the IRS reflection coefficient. Constraint (6g) represents the combination set of all possible decoding orders.

For the OMA scheme, the optimization problem is formulated as

$$(\mathbf{P2}) \quad \max_{p_1(i), p_2(i), \Theta} \quad \mathbb{E}_i[R_1^{\text{OMA}}(i) + R_2^{\text{OMA}}(i)] \quad (7a)$$

$$\text{s.t.} \quad (6b), (6c), (6d), (6e), (6f). \quad (7b)$$

B. Phase Shift Adjustment

1) *NOMA*: With given transmit power in corresponding phase adjustment schemes, we can obtain the phase shifts Θ for the NOMA scheme by solving

$$(\mathbf{P1.1}) \quad \max_{\Theta} \quad \mathbb{E}_i[R_1^{\text{NOMA}}(i) + R_2^{\text{NOMA}}(i)] \quad (8a)$$

$$\text{s.t.} \quad (6e), (6f). \quad (8b)$$

The problem is a complicated optimization problem. The non-convexity is presented by its non-convex objective function and a discrete unit-modulus constraint on reflecting elements. The globally optimal solution is hard to obtain by efficient methods or tools. One way to reach the globally optimal phase shifts is exhaustive search. Specifically, all the possible cases of Θ are established and one Θ is then chosen, which achieves the maximum data rate. However, brute-force search method can lead to exponential complexity with $O(L^N)$, which is time consuming if the sizes of N and L are large. Therefore, we only use the exhaustive search as the upper bound and a benchmark for our proposed methods.

Considering aforementioned reasons, we propose efficient algorithms that can achieve the near optimal performance, but with low computational complexity. Particarliy, the alternating

optimization (AO) method is utilized. First, let $I_k = \text{diag}(r_k^H)G$, $\bar{u} = [u, 1]$, and we introduce

$$Z_k = \begin{bmatrix} I_k \\ h_k^H \end{bmatrix}. \quad (9)$$

Then we can obtain $|h_k + r_k^H \Theta G|^2 = |\bar{u}Z_k|^2$. Let $\frac{1}{X_{kj}} = |\bar{u}Z_k|^2 p_j$ and $Y_{kj} = |\bar{u}Z_k|^2 p_j + \sigma^2$. Given the decoding order, i.e., $\Omega(1) < \Omega(2)$, problem (P1.1) can be transformed into a more tractable form

$$(\mathbf{P1.1.1}) \max_{\Theta} \mathbb{E}_i[R_1^{\text{NOMA}}(i) + R_2^{\text{NOMA}}(i)] \quad (10a)$$

$$\text{s.t.} \quad \log_2\left(1 + \frac{1}{X_{11}Y_{12}}\right) \geq \bar{R}, \quad (10b)$$

$$\log_2\left(1 + \frac{1}{X_{22}\sigma^2}\right) \geq \bar{R}, \quad (10c)$$

$$\frac{1}{X_{kk}} \leq |\bar{u}Z_k|^2 p_k, \quad k = 1, 2, \quad (10d)$$

$$Y_{12} \geq |\bar{u}Z_1|^2 p_2 + \sigma^2, \quad (10e)$$

$$|\bar{u}_n|^2 = 1, \forall n. \quad (10f)$$

The constraints (10b), (10d), and (10f) are non-convex. Note that $\log_2(1 + \frac{1}{XY})$ is a joint convex function with respect to X and Y . Then the lower bound at given local points $\{X_{11}, Y_{12}\}$ can be achieved by utilizing the first-order Taylor expansion. Correspondingly, the lower bound of the weak user and strong user can be expressed as

$$\log_2\left(1 + \frac{1}{X_{11}Y_{12}}\right) \geq R_1^{\text{low}}, \quad (11)$$

and

$$\log_2\left(1 + \frac{1}{X_{22}\sigma^2}\right) \geq R_2^{\text{low}}, \quad (12)$$

respectively, where

$$\begin{aligned} R_1^{\text{low}} &= \log_2\left(1 + \frac{1}{X_{11}(l)Y_{12}(l)}\right) - \\ &\quad \frac{(\log_2^e)(X_{11} - X_{11}(l))}{X_{11}(l) + X_{11}(l)^2 Y_{12}(l)} - \frac{(\log_2^e)(Y_{12} - Y_{12}(l))}{Y_{12}(l) + Y_{12}(l)^2 X_{11}(l)}, \end{aligned} \quad (13)$$

and

$$R_2^{low} = \log_2\left(1 + \frac{1}{X_{22}(l)\sigma^2}\right) - \frac{(\log_2^e)(X_{22} - X_{22}(l))}{\sigma^2(X_{22}(l) + X_{22}(l)^2\sigma^2)}. \quad (14)$$

Then the term on the right side of (10d) is a convex function with respect to \bar{u} . Similarly, at the given local point $\bar{u}(l)$, the lower bound achieved by utilizing first-order Taylor expansion can be given by

$$|\bar{u}Z_k|^2 \geq \delta_k = |\bar{u}(l)Z_k|^2 + 2\mathcal{R}e((\bar{u}(l)Z_kZ_k^H)(\bar{u} - \bar{u}(l))). \quad (15)$$

Thus, the phase shifters adjustment problem can be approximated as

$$\begin{aligned} \mathbf{(P1.1.2)} \quad \max_{\Theta} \quad & \mathbb{E}_i[R_1^{\text{NOMA}}(i) + R_2^{\text{NOMA}}(i)] \end{aligned} \quad (16a)$$

$$\text{s.t.} \quad R_k^{low} \geq \bar{R}, \quad k = 1, 2, \quad (16b)$$

$$\frac{1}{X_{kk}} \leq \delta_k p_k, \quad k = 1, 2, \quad (16c)$$

$$Y_{12} \geq |\bar{u}Z_1|^2 p_2 + \sigma^2, \quad (16d)$$

$$|\bar{u}_n|^2 = 1, \forall n, \bar{i}_{n+1} = 1. \quad (16e)$$

The non-convexity still lies in the rank-one constraint (16e). One common method is applying semidefinite relaxation (SDR), where the rank-one constraint is first ignored and a solution with random rank is obtained. Then the solution is constructed to the rank-one form by applying Gaussian randomization method. Although dropping the rank-one constraint could lead to a relaxed convex problem, the obtained solution is usually sub-optimal. To overcome this challenge, a novel algorithm based on sequential rank-one constraint relaxation (SROCR) is applied. Particularly, we define $U = \bar{u}\bar{u}^H$, where $U \succeq 0$, $\text{rank}(U) = 1$ and $[U]_{nn} = 1$. Then the problem

(P1.1.2) is reformulated into

$$(\mathbf{P1.1.3}) \max_{\Theta} \mathbb{E}_i[R_1^{\text{NOMA}}(i) + R_2^{\text{NOMA}}(i)] \quad (17a)$$

$$\text{s.t.} \quad R_k^{low} \geq \bar{R}, \quad k = 1, 2, \quad (17b)$$

$$\frac{1}{X_{kk}} \leq \text{Tr}(UZ_kZ_k^H)p_k, \quad k = 1, 2, \quad (17c)$$

$$Y_{12} \geq \text{Tr}(UZ_1Z_1^H)p_2 + \sigma^2, \quad (17d)$$

$$U \succeq 0, \quad (17e)$$

$$\text{rank}(U) = 1, \quad (17f)$$

$$[U]_{nn} = 1. \quad (17g)$$

We first apply a partial constraint relaxation for the (17f) and the relaxed problem (P1.1.3) is given by

$$(\mathbf{P1.1.4}) \max_{\Theta} \mathbb{E}_i[R_1^{\text{NOMA}}(i) + R_2^{\text{NOMA}}(i)] \quad (18a)$$

$$\text{s.t.} \quad e_{\max}(U^{(i)})^H U e_{\max}(U^{(i)}) \geq \kappa^{(i)} \text{Tr}(U), \quad (18b)$$

$$(17b), (17c), (17d), (17e), \quad (18c)$$

where $\kappa^{(i)} \in [0, 1]$ is the relaxation parameter, $U^{(i)}$ denotes the largest eigenvalue of U and $e_{\max}(U^{(i)})$ denotes the eigenvector of the $U^{(i)}$. $\kappa^{(i)}$ controls the largest eigenvalue to trace ratio of U , as the solution $U^{(i)}$ in the i -th iteration. The problem (P1.1.4) is a convex problem, which can be solved efficiently by the standard convex optimization tools, such as CVX. When $\kappa^{(i)} = 0$, constraint (18b) could be considered as dropping the rank-one constraint, while $\kappa^{(i)} = 1$, constraint (18b) approaches to the original rank-one constraint in (17f). Note that due to the relaxation replacement, the solution of problem (P1.1.4) serves as the lower bound of problem (P1.1). Then, we apply Cholesky decomposition, e.g. $U^{l+1} = \bar{u}\bar{u}^H$, to find the phase shifters. Algorithm 1 summarizes the proposed algorithm to solve problem (P1.1.3).

Theorem 1. With initial solution of phase shifts, Algorithm 1 converges to a KKT stationary point of problem (P1.1.4), which is equivalent to problem (P1.1.3).

Proof: The algorithm to build a rank one solution can be considered as an AO of $u =$

Algorithm 1 Proposed algorithm for NOMA phase adjustment

```

1: Initialize: Convergence thresholds  $\epsilon_1, \epsilon_2$ , a feasible solution  $U(l)$ , step size  $\Delta^{(i)}$  and iteration index  $i = 0$ .
2: Solve problem (P1.1.4) and obtain  $u^{(i)}$  with  $\kappa(i) = 0$ .
3: repeat
4:   Solve problem (P1.1.4) with  $\{\kappa^{(i),U^{(i)}}\}$ .
5:   if  $\{\kappa^{(i),U^{(i)}}\}$  is feasible then
6:     Obtain the optimal solution  $\overline{U}^{(l+i)}$ ,
7:      $\Delta^{(i+1)} = \Delta^{(i)}$ ;
8:   else
9:      $\Delta^{(i+1)} = \Delta^{(i)}/2$ ;
10:  end
11:   $\kappa^{(i+1)} = \min(1, \frac{e_{\max}(U^{(i+1)})}{Tr(\overline{U}^{(l+i)})} + \Delta^{(i+1)})$ .
12:   $i = i + 1$ .
13: until  $\kappa^{(i-1)} \geq \epsilon_1$  and objective value with the obtained  $U$  reaches convergence with  $\epsilon_2$ .
  
```

$e_{\max}(U^{(i)})$ and U . The proof is detailed in [44]. ■

The obtained solution u is still continuous. The nearest feasible discrete phase shifters are obtained by quantizing as

$$u^* = \begin{cases} e^{j\theta_n^*}, & n = 1, \dots, N, \\ 1 & n = N + 1, \end{cases} \quad (19)$$

where

$$\theta_n^* = \operatorname{argmin} |\theta - \operatorname{angle}(u)|. \quad (20)$$

Note that the newly obtained solution u^* may not be locally optimal, thus solution u^* is updated only when the objective functions value increases. In the following, two types of multiple access schemes, namely. FDMA and TDMA, are consider in both dynamic phase adjustment and one-time phase adjustment schemes.

2) *OMA*: Since the IRS is to be optimised for maximising the sum rate of two users at the same time under both the FDMA and TDMA schemes in the one-time phase adjustment scheme,

the formulation becomes

$$\mathbf{(P2.1)} \max_{\Theta} \mathbb{E}_i[R_1^{\text{OMA}}(i) + R_2^{\text{OMA}}(i)] \quad (21a)$$

$$\text{s.t.} \quad (6e), (6f). \quad (21b)$$

Similarly, we introduce the slack variables $\frac{1}{X_{kj}} = |\bar{u}W_k|^2 p_j$ and $U = \bar{u}\bar{u}^H$, then problem (P2.1) is reformulated as

$$\mathbf{(P2.1.1)} \max_{\Theta} \mathbb{E}_i[R_1^{\text{OMA}}(i) + R_2^{\text{OMA}}(i)] \quad (22a)$$

$$\text{s.t.} \quad \log_2\left(1 + \frac{1}{X_{kk}\sigma^2}\right) \geq \bar{R}, \quad \forall k = 1, 2, \quad (22b)$$

$$\frac{1}{X_{kk}} \leq \text{Tr}(UZ_kZ_k^H)p_k, \quad k = 1, 2, \quad (22c)$$

$$U \succeq 0, \quad (22d)$$

$$\text{rank}(U) = 1, \quad (22e)$$

$$[U]_{nn} = 1. \quad (22f)$$

By substituting (11), (12) and (15), the passive beamforming optimization problem under the OMA scheme is approximated as

$$\mathbf{(P2.1.2)} \max_{\Theta} \mathbb{E}_i[R_1^{\text{OMA}}(i) + R_2^{\text{OMA}}(i)] \quad (23a)$$

$$\text{s.t.} \quad R_k^{\text{low}} \geq \bar{R}, \quad k = 1, 2, \quad (23b)$$

$$(22c), (22d), (22e), (22f). \quad (23c)$$

We also use the SROCR to solve the rank-one constraint as

$$\mathbf{(P2.1.3)} \max_{\Theta} \mathbb{E}_i[R_1^{\text{NOMA}}(i) + R_2^{\text{NOMA}}(i)] \quad (24a)$$

$$\text{s.t.} \quad e_{\max}(U^{(i)})^H U e_{\max}(U^{(i)}) \geq \kappa^{(i)} \text{Tr}(U), \quad (24b)$$

$$(22c), (22d), (22f), (23b). \quad (24c)$$

Now, problem (P2.1.3) is also convex, then the algorithm for phase adjustment under OMA scheme is summarized in Algorithm 2.

Algorithm 2 Proposed algorithm for OMA phase adjustment

```

1: Initialize: Convergence thresholds  $\epsilon_1, \epsilon_2$ , a feasible solution  $U(l)$ , step size  $\Delta^{(i)}$  and iteration
   index  $i = 0$ ;
2: Solve problem (P2.1.3) and obtain  $u^{(i)}$  with  $\kappa(i) = 0$ .
3: repeat
4:   Solve problem (P2.1.3) with  $\{\kappa^{(i),U^{(i)}}\}$ .
5:   if  $\{\kappa^{(i),U^{(i)}}\}$  is feasible then
6:     Obtain the optimal solution  $\bar{U}^{(l+i)}$ ,
7:      $\Delta^{(i+1)} = \Delta^{(i)}$ ;
8:   else
9:      $\Delta^{(i+1)} = \Delta^{(i)}/2$ ;
10:  end
11:   $\kappa^{(i+1)} = \min(1, \frac{e_{\max}(U^{(i+1)})}{Tr(U^{(i+1)})} + \Delta^{(i+1)})$ .
12:   $i = i + 1$ .
13: until  $\kappa^{(i-1)} \geq \epsilon_1$  and objective value with the obtained  $U$  reaches convergence with  $\epsilon_2$ .

```

3) *TDMA under dynamic phase adjustment scheme*: In the dynamic scheme, we are aiming at maximising each user's concatenated channel response $h_k(i) + r_k^H(i)\Theta G(i)$, as the IRS could be optimised for one user in different time slots. Given a transmit power allocation, the problem (P1) satisfies the following inequality:

$$|h_k(i) + r_k^H(i)\Theta G(i)| \stackrel{(a)}{\leq} |h_k(i)| + |r_k^H(i)\Theta G(i)|, \quad (25)$$

where the equality in (a) holds if and only if $\arg(r_k^H(i)\Theta G(i)) = \arg(h_k(i)) = \phi_0$. We can always obtain a phase shifter Θ that satisfies (a) with equality. By changing the variables of $r_k^H(i)\Theta G(i) = v^H a$, where $a = \text{diag}(r_k^H G(i))$, and droping the constant term $h_k(i)$, we arrive at the following simplified problem

$$(\mathbf{P2.2}) \max_v |v^H a| \quad (26a)$$

$$\text{s.t.} \quad 0 \leq \theta_n \leq 2\pi, \forall n, \quad (26b)$$

$$\arg(v^H a) = \phi_0. \quad (26c)$$

The optimal solution for problem (P2.2) can be obtained by

$$v^* = e^{j(\phi_0 - \arg(a))} = e^{j(\phi_0 - \arg(\text{diag}(r_k^H(i))G(i)))}. \quad (27)$$

The n -th phase shifter at the IRS can be expressed as

$$\begin{aligned}\theta_n^* &= \phi_0 - \arg(r_{n,k}^H(i)G_n(i)) \\ &= \phi_0 - \arg(r_{n,k}^H(i)) - \arg(G_n(i)),\end{aligned}\tag{28}$$

where $r_{n,k}^H(i)$ denotes the n -th element of $r_k^H(i)$, and $G_n(i)$ denotes the n th element of $G(i)$. Equation (28) suggests the optimal phase shifts solution is that the reflection links and direct links is aligned with BS-user link to maximise the concatenated channel response for each user. Then, we optimize the power allocation as well as the time or frequency allocation in OMA schmems under given phase shifter Θ in the following section.

C. Power Allocation

1) *Optimal Solution to NOMA Scheme:* With given phase shifter Θ and minimum achievable rates \bar{R} , our objective is maximizing the system average sum rate in each fading state or fading block. We optimize the power allocation, subject to power budget constraints. The target rate for both users is also considered for ensure the fairness between the users. Thus the objective function is rewritten as follows

$$\mathbf{(P1.2)} \quad \max_{p_1(i), p_2(i)} \quad \mathbb{E}_i[R_1^{\text{NOMA}}(i) + R_2^{\text{NOMA}}(i)] \tag{29a}$$

$$\text{s.t.} \quad (6b), (6c), (6d), (6e), (6g). \tag{29b}$$

We fix the reflection coefficients and decoding order in each fading state or fading block, then we solve the power allocation problem. The objective function of problem (P1.2) is non-convex. Thus the optimal solution is hard to obtained by efficient methods. The problem (P1.2) satisfies the time-sharing condition, which is always satisfied when the number of fading states goes to infinity [45]. Strong duality holds when such condition is met. By using the Lagrangian duality, the duality gap between the original and the dual problems ecomes zero when time-sharing condition is satisfied by problem (P1.2). Hence, we can obtain the optimal solution of problem (P1.2) by solving its dual problem. Then, the Lagrange duality method can be utilized to obtain

the solution of problem (P1.2). The Lagrangian function of the primal problem is given by

$$\begin{aligned}\mathcal{L}_{dt}^{\text{NOMA}}(\{p_1(i)\}, \{p_2(i)\}, \lambda, \delta, \mu) = \\ \mathbb{E}_i[(1 + \delta)R_1^{\text{NOMA}}(i) + (1 + \mu)R_2^{\text{NOMA}}(i) \\ - \lambda(p_1(i) + p_2(i))] + \lambda\bar{P} - \delta\bar{R} - \mu\bar{R},\end{aligned}\quad (30)$$

where λ is the non-negative Lagrange multipliers for the constraint (6b), δ and μ are associated with constraints (6e) for user 1 and user 2, respectively. Accordingly, the Lagrange dual function can be expressed as

$$\begin{aligned}\mathcal{D}_{dt}^{\text{NOMA}}(\lambda, \delta, \mu) \\ = \max_{\{p_1(i), p_2(i)\}} \mathcal{L}_{dt}^{\text{NOMA}}(\{p_1(i)\}, \{p_2(i)\}, \lambda, \delta, \mu).\end{aligned}\quad (31)$$

The dual of problem (P1.2) is then formulated as

$$\begin{aligned}\mathbf{(D1)} \quad \min_{\lambda, \delta, \mu} \quad \mathcal{D}_{dt}^{\text{NOMA}}, \\ \text{s.t.} \quad \lambda \geq 0, \delta \geq 0, \mu \geq 0.\end{aligned}\quad (32)$$

The optimal solution for dual problem (D1) is equivalent to that for problem (P1.2), when the strong duality holds under time-sharing condition. In the following, we first obtain $\mathcal{D}_{dt}^{\text{NOMA}}(\lambda, \delta, \mu)$ from (31), then decouple problem (D1) into multiple subproblems, and each subproblem denotes one fading state in the entire process. Consider one particular fading state with given (λ, δ, μ) , the index i can be ignored and the subproblem is given by

$$\begin{aligned}\mathbf{(D1.1)} \quad \max_{p_1 \geq 0, p_2 \geq 0} \quad \bar{\mathcal{L}}_{dt}^{\text{NOMA}}(p_1, p_2), \\ \text{s.t.} \quad p_1 + p_2 \leq \hat{P},\end{aligned}\quad (33)$$

where $\bar{\mathcal{L}}_{dt}^{\text{NOMA}}(p_1, p_2) = (1 + \delta)R_1^{\text{NOMA}} + (1 + \mu)R_2^{\text{NOMA}} - \lambda(p_1 + p_2)$. Since all fading states are independent, all the subproblems can be solved parallelly. Therefore, we focus on solving problem (D1.1) in the sequel.

Proposition 1. When $g_1 > g_2$, the optimal solution for problem (D1.1) is given by

$$\{p_1^*, p_2^*\} = \operatorname{argmax} \{\bar{L}_{dt}^{NOMA}(0, 0), \bar{L}_{dt}^{NOMA}(0, \hat{P}), \bar{L}_{dt}^{NOMA}(\hat{P}, 0), \bar{L}_{dt}^{NOMA}(p_{i,1}, p_{i,2})\}, \quad (34)$$

where $(p_{i,1}, p_{i,2}), i \in \{1, 2, 3, 4\}$ are the corresponding solution pair given as

$$\begin{cases} p_{1,1} = 0, & p_{1,2} = \left[\frac{1+\mu}{\lambda \ln 2} - \frac{1}{g^2} \right]_0^{\hat{P}}, \\ p_{2,1} = \left[\frac{1+\delta}{\lambda \ln 2} - \frac{1}{g^1} \right]_0^{\hat{P}}, & p_{2,2} = 0, \\ p_{3,1} = \left[\frac{(1+\mu)/g_1 - (1+\delta)/g_2}{\delta - \mu} \right]_0^{\hat{P}}, & \\ p_{3,2} = \left[\hat{P} - \frac{(1+\mu)/g_1 - (1+\delta)/g_2}{\delta - \mu} \right]_0^{\hat{P}}, & \\ p_{4,1} = \frac{(1+\mu)/g_1 - (1+\delta)/g_2}{\delta - \mu}, & \\ p_{4,2} = \frac{1+\mu}{\lambda \ln 2} - \frac{1}{g^2} - \frac{(1+\mu)/g_1 - (1+\delta)/g_2}{\delta - \mu}. & \end{cases} \quad (35)$$

Proof: Since $\bar{L}_{dt}^{NOMA}(p_1, p_2)$ is a continuous function over $\psi = \{(p_1, p_2) | p_1 \geq 0, p_2 \geq 0, p_1 + p_2 \leq \hat{P}\}$, its maximum proves to be either at the stationary point or on the boundary of ψ when the stationary point is infeasible. The stationary point $(p_{4,1}, p_{4,2})$ is given by

$$(p_{4,1}, p_{4,2}) = \arg \{ \nabla_{(p_1, p_2)} \bar{L}_{dt}^{NOMA}(p_1, p_2) = 0 \}. \quad (36)$$

If $(p_{4,1}, p_{4,2}) \in \psi$, the maximum is obtained by $\bar{L}_{dt}^{NOMA}(p_{4,1}, p_{4,2})$, otherwise the maximum can be obtained by the boundary lies in $p_1 = 0, p_2 = 0$ or $p_1 + p_2 = \hat{P}$. Each boundary is denoted by $(p_{i,1}, p_{i,2}), i \in \{1, 2, 3\}$, respectively. \blacksquare

We can find \mathcal{D}_{dt}^{NOMA} efficiently by solving all sub-problems (D1.1) in parallel with given (λ, δ, μ) . The subgradient-based methods, such as the deep-cut ellipsoid method, can be applied to solve the dual problem [46]. The problem (D1) sub-gradient for updating (λ, δ, μ) is given by $(\bar{P} - \mathbb{E}_i[p_1^*(i) + p_2^*(i)], \mathbb{E}_i[R_1^{*NOMA}(i)] - \bar{R}, \mathbb{E}_i[R_2^{*NOMA}(i)] - \bar{R})^T$, where $(p_1^*(i), p_2^*(i))$ is the optimal solution to (D1), and $R_k^{*NOMA}(i)$ is obtained by substituting the solution into (4).

The overall procedure for solving the problem (P1) is summarized in Algorithm 3.

Algorithm 3 Iterative algorithm for problem (P1)

- 1: **Initialize:** Feasible solutions $\{p_k\}$ and phase shifter $\{u(l)\}$;
- 2: Iteration count $l = 0$;
- 3: **repeat**
- 4: Solve problem (P1.2) with given u and obtained the optimal $\{p_k^{(l+1)}\}$.
- 5: Solve problem (P1.1.1) by algorithm 1 and obtained phase shifter $\{u^{(l+1)}\}$.
- 6: Obtain the discrete feasible solution u^* via (19).
- 7: **if** objective value increases, **then**
- 8: $\{u^{(l+1)}\} = u^*$;
- 9: **else**
- 10: $u^{(l+1)} = u^{(l)}$;
- 11: **end**
- 12: $l = l + 1$.
- 13: **until** The objective value convergence with the threshold $\epsilon > 0$.

2) *Optimal Solution to OMA Schemes:* The power allocation problem for the OMA schemes is described as follows:

$$(\mathbf{P2.3}) \quad \max_{p_1(i), p_2(i)} \mathbb{E}_v[R_1^{\text{OMA}}(i) + R_2^{\text{OMA}}(i)] \quad (37a)$$

$$\text{s.t.} \quad (6b), (6c), (6d), (6e). \quad (37b)$$

The convexity still lies in problem (P2.3), since $\alpha_k(i) \log_2(1 + p_k(i)g_k(i))$ is jointly concave with respect to $\alpha_k(i)$ and $p_k(i)$. Then, for the strong duality, the Lagrangian dual method is applied for solving problem (P2.3) and the Lagrangian function is given by

$$\begin{aligned} \mathcal{L}_{dt}^{\text{OMA}}(\{p_1(i)\}, \{p_2(i)\}, \{\alpha_1(i)\}, \lambda, \delta, \mu) = \\ \mathbb{E}_i[(1 + \delta)R_1^{\text{OMA}}(i) + (1 + \mu)R_2^{\text{OMA}}(i) \\ - \lambda(p_1(i) + p_2(i))] + \lambda\bar{P} - \delta\bar{R} - \mu\bar{R}, \end{aligned} \quad (38)$$

where λ, δ and μ are the non-negative Lagrange multipliers similar with those in NOMA scheme, and $\alpha_2 = 1 - \alpha_1$. Similarly, we can decouple $\mathcal{L}_{dt}^{\text{OMA}}(\{p_1(i)\}, \{p_2(i)\}, \{\alpha_1(i)\}, \lambda, \delta, \mu)$ into parallel sub-Lagrangian for the same structure, with $\bar{\mathcal{L}}_{dt}^{\text{OMA}}(p_1, p_2, \alpha_1) = (1 + \delta)R_1^{\text{OMA}} + (1 + \mu)R_2^{\text{OMA}} - \lambda(p_1 + p_2)$, where the fading state index i has been ignored as sub-problems are considered in each fading state. Then, one particular sub-problem corresponding a single fading state is

formulated as

$$\begin{aligned}
 \mathbf{(D2)} \quad & \max_{p_1 \geq 0, p_2 \geq 0, \alpha_1} \bar{\mathcal{L}}_{dt}^{\text{OMA}}(p_1, p_2, \alpha_1), \\
 & \text{s.t.} \quad p_1 + p_2 \leq \hat{P}, \\
 & \quad 0 \leq \alpha_1 \leq 1.
 \end{aligned} \tag{39}$$

Lemma 1. If the maximum of $\bar{\mathcal{L}}_{dt}^{\text{OMA}}(p_1, p_2, \alpha_1)$ is achieved by the jointly stationary point, the following conditions should be satisfied:

$$h(\lambda, \theta, \mu) = 0, \tag{40a}$$

$$c_1 \leq 0, \tag{40b}$$

$$c_2 \leq 0, \tag{40c}$$

$$\begin{cases} \frac{\hat{P}-c_2}{c_1-c_2} \leq 0, & \text{if } c_1 \leq c_2, \\ \frac{\hat{P}-c_2}{c_1-c_2} \geq 1, & \text{otherwise,} \end{cases} \tag{40d}$$

where $c_1 = \frac{1+\delta}{\lambda \ln 2} - \frac{1}{g_1}$, $c_2 = \frac{1+\mu}{\lambda \ln 2} - \frac{1}{g_2}$ and $h(\lambda, \theta, \mu)$ is given by

$$\begin{aligned}
 h(\lambda, \theta, \mu) = & (1 + \delta) \log_2 \left(\frac{1 + \delta}{\lambda \ln 2} g_1 \right) \\
 & - (1 + \mu) \log_2 \left(\frac{1 + \mu}{\lambda \ln 2} g_2 \right) - \lambda c_1 + \lambda c_2.
 \end{aligned} \tag{41}$$

The stationary point is thus given by

$$p_1^* = c_1 \alpha_1^*, \quad p_2^* = c_2 \alpha_2^* \tag{42a}$$

$$\alpha_1^* = \begin{cases} \forall \in [0, \min\{\frac{\hat{P}-c_2}{c_1-c_2}, 1\}], & \text{if } c_1 > c_2 \\ \forall \in [(\frac{\hat{P}-c_2}{c_1-c_2})^+, 1\}], & \text{otherwise.} \end{cases} \tag{42b}$$

Proof: The jointly stationary point is achieved by solving $\nabla_{(p_1, p_2, \alpha_1)} \bar{\mathcal{L}}_{dt}^{\text{OMA}}(p_1, p_2, \alpha_1) = 0$, and (40a) is obtained by plugging $p_1 = c_1 \alpha_1$ and $p_2 = c_2 \alpha_2$ into the partial derivative $\bar{\mathcal{L}}_{dt}^{\text{OMA}}(p_1, p_2, \alpha_1)$ with respect to α_1 . Then, considering $p_1 \leq 0$, $p_2 \leq 0$ and $p_1 + p_2 \geq \hat{P}$, we have (40b), (40c) and (40d) denotes the feasible range for α_1 , respectively. \blacksquare

If $\bar{\mathcal{L}}_{dt}^{\text{OMA}}(p_1, p_2, \alpha_1)$ achieves the maximum on the boundary points where $p_1 + p_2 = \hat{P}$, the

optimum (p_1, p_2, α_1) should be

$$\begin{cases} p_1^* = 0, p_2^* = \hat{P}, \alpha_1^* = 0, & \text{if } \frac{1+\mu}{1+\delta} > \frac{\log_2(1+\hat{P}g_1)}{\log_2(1+\hat{P}g_2)}, \\ p_1^* = \hat{P}, p_2^* = 0, \alpha_1^* = 1, & \text{otherwise.} \end{cases} \quad (43)$$

The optimal solution to problem (D2) is thus given by

$$\begin{aligned} (p_1^*, p_2^*, \alpha_1^*) = & \operatorname{argmax} \{ \bar{\mathcal{L}}_{dt}^{\text{OMA}}(0, 0, 0), \\ & \bar{\mathcal{L}}_{dt}^{\text{OMA}}(0, \hat{P}, 0), \bar{\mathcal{L}}_{dt}^{\text{OMA}}(\hat{P}, 0, 1), \\ & \bar{\mathcal{L}}_{dt}^{\text{OMA}}(0, c_2, 0), \bar{\mathcal{L}}_{dt}^{\text{OMA}}(c_1, 0, 1) \}, \end{aligned} \quad (44)$$

Problem (D2) is solved by solving the subproblems with given (λ, δ, μ) . The sub-gradient method is also applied with the corresponding sub-gradient $(\bar{P} - \mathbb{E}_v[p_1^*(i) + p_2^*(i)], \mathbb{E}_v[R_1^{*OMA}(i)] - \bar{R}, \mathbb{E}_v[R_2^{*OMA}(i)] - \bar{R})^T$ for updating (λ, δ, μ) . Then, problem (P2.3) is iteratively solved and the overall algorithm for the IRS-aided OMA scheme is summarized in Algorithm 4.

Algorithm 4 Iterative algorithm for problem (P2)

- 1: **Initialize:** Feasible solutions $\{p_k\}$ and phase shifter $\{u(l)\}$;
- 2: Iteration count $l = 0$;
- 3: **repeat**
- 4: Solve problem (P2.2) with given u and obtained the optimal $\{p_k^{(l+1)}\}$.
- 5: Solve problem (P2.1) or problem (P2.2) obtained phase shifter $\{u^{(l+1)}\}$.
- 6: Obtain the discrete feasible solution u^* via (19).
- 7: **if** objective value increases, **then**
- 8: $\{u^{(l+1)}\} = u^*$;
- 9: **else**
- 10: $u^{(l+1)} = u^{(l)}$;
- 11: **end**
- 12: $l = l + 1$.
- 13: **until** The objective value convergence with the threshold $\epsilon > 0$.

D. Complexity and Convergence

The AO method is applied for problems (P1) and (P2) and detailed in Algorithms 3 and 4. The proposed phase shifters adjustment algorithms contain interior-point method, and the complexity is given by $\mathcal{O}(I^s(3k^2 + N^2)^{3.5})$, where I^s defines the iteration number of the SROCR method in

Algorithms 1 and 2. The convergence of Algorithms 1 and 2 is similar and we take Algorithm 1 for example. With given power, time and frequency allocations for problem (P1.1), we have

$$\begin{aligned}
 x(\{p_k^l\}, u^l) &\stackrel{(a)}{=} x^{lb}(\{p_k^l\}, u^l) \\
 &\stackrel{(b)}{\leq} x^{lb}(\{p_k^{l+1}\}, u^{l+1}) \\
 &\stackrel{(c)}{\leq} x(\{p_k^{l+1}\}, u^{l+1}),
 \end{aligned} \tag{45}$$

where x^{lb} denotes the problem (P1.1.2)s value in l-th iteration. With given local points in problem (P1.1.2), the first-order Taylor expansions are tight and (a) holds. Due to "time-sharing" condition is satisfied, problem (P1.2) is solved with optimal solution and (b) holds. Since relaxation replacement for rank-one constrain, (c) holds. As a result, the obtained problem (P1.1)s value remains non-decreasing in each iteration. Then, we have

$$x(\{p_k^l\}, u^l) \leq x(\{p_k^{l+1}\}, u^{l+1}). \tag{46}$$

Remark 2. *The maximum is bounded by a finite value. The proposed algorithms always converge to a locally optimal solution for both problems (P1) and (P2) as shown in Equation (46).*

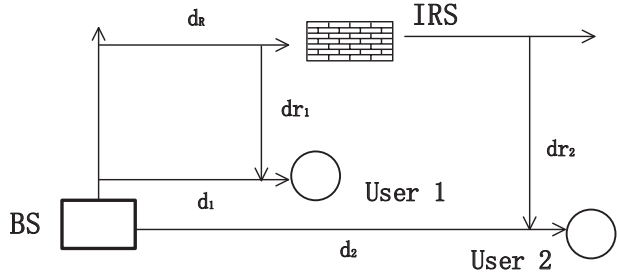


Fig. 2: The simulated IRS-assisted network.

IV. SIMULATION RESULTS

In this section, numerical results are persented for verifying our proposed algorithms. The downlink IRS-assisted system over fading channels is illustrated in Fig. 2. The BS and the IRS's locations are at $(0, 0, 0)$ and $(70, 0, 0)$, respectively. We randomly set users' locations, which are deployed around the BS or the IRS. The BS-user distance are set to 100m and 200m, the IRS-user distance are set to 70m and 140m. The rayleigh fading channel model is modeled for

the direct link and the rician fading model is modeled for the assistant link. Let v_{BU} and v_{UI} denote the Rician factors of the BS-IRS and IRS-user links, where $v_{BI} = v_{IU} = 3dB$. The path loss exponents for the BS-user, BS-IRS, and IRS-user links are set to be $\varphi_{BU} = 3.5$, $\varphi_{BI} = 2.2$ and $\varphi_{IU} = 2.8$, respectively. The convergence threshold is $\xi = 10^{-2}$ and the noise power is set as $\sigma^2 = -90dBm$. The number of fading states is set as $N = 10^7$ for the approximate infinity.

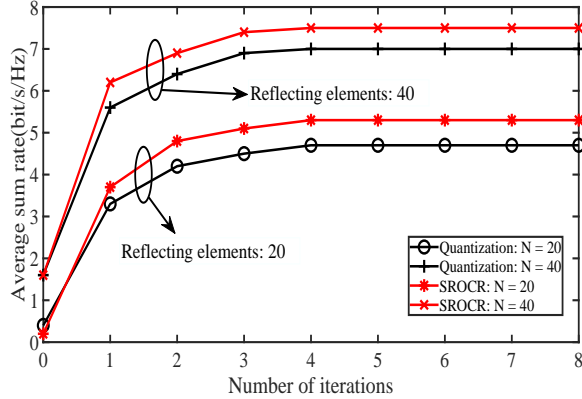


Fig. 3: The average sum rate versus number of iterations.

The convergence of the SROCR with/without quantization versus iteration numbers:

Fig. 3 illustrates the achieved sum rate versus the number of iterations required by proposed algorithms. We randomly generate continuous phase shifts as the initial solution. Then we obtain the discrete phase shifts by quantizing. Fig 3 shows that with a small number of iterations, proposed algorithms can converge, which verifies the insights gleaned from **Remark 2**. Thus we can build a feasible rank one solution efficiently.

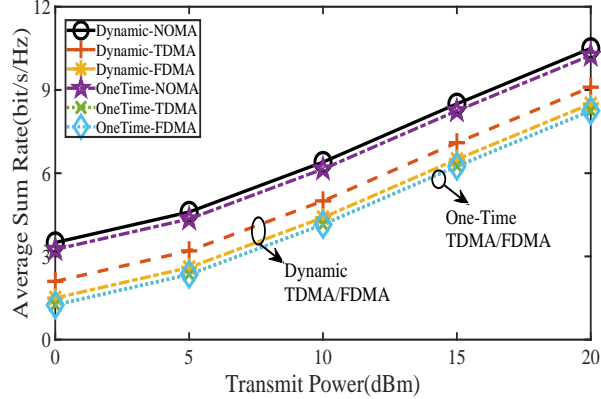


Fig. 4: The average sum rate versus transmit power under various phase adjustment.

Average sum rate versus transmit power under various phase adjustment: As shown in Fig. 4, the performance in the dynamic phase adjustment scheme outperforms the one-time phase adjustment scheme, as the reflecting elements are optimised in every fading state. The gain of adjusting the phase shift in every fading state is not pronounced while the complexity and the power for adjusting the reflecting elements increases significantly. The IRS-assisted NOMA scheme outperforms OMA scheme under both dynamic phase adjustment and one-time phase adjustment. In addition, for the hardware limitation of the elements on IRS, IRS has the feature of time-selective, while frequency-selective can not be achieved by the phase shifters. The TDMA scheme outperforms the FDMA scheme under dynamic phase adjustment for the proposed system, which validates our **Remark 1**.

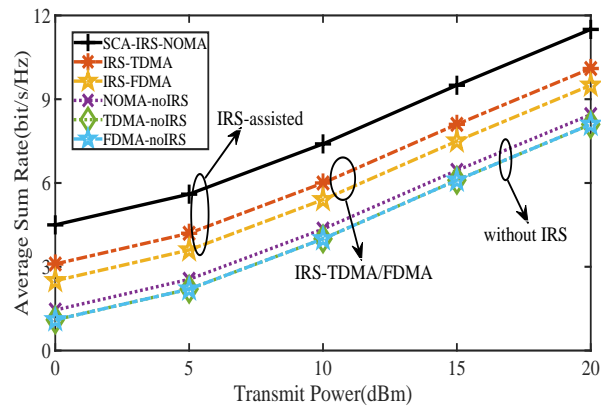


Fig. 5: The average sum rate versus transmit power under dynamic phase adjustment.

Average sum rate versus transmit power under dynamic phase adjustment: As shown in Fig. 5, the system average sum rate versus the power budget under different schemes. The number of IRS elements is set to $N = 30$. Under various multiple access schemes, the average sum rate increases with the higher transmit power. Compared to the traditional NOMA scheme, the performance gain comes from the enhanced combined-channel introduced by the IRS. Moreover, larger channel condition differences can be achieved for the IRS has the ability to adjust the propagation environment. Besides, NOMA scheme can achieve higher average throughput in comparison with the OMA scheme. As NOMA allows multiple users to share the same resource block, the higher spectral efficiency can be obtained.

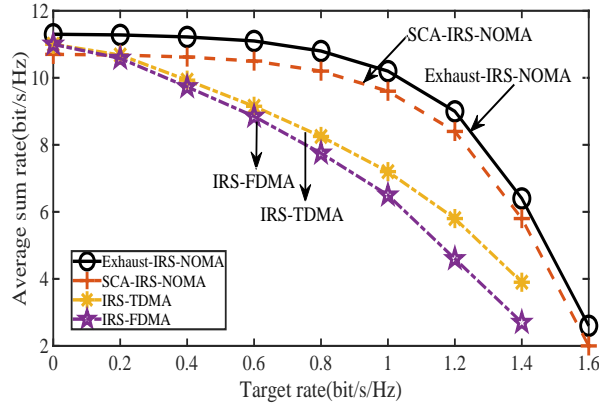


Fig. 6: The average sum rate versus users target rate under dynamic phase adjustment.

Average sum rate versus users target rate under dynamic phase adjustment: Fig. 6 depicts the relationships between the average rate performance of the network and the users fairness, obtained from NOMA and OMA schemes assisted by IRS. It can be seen that the IRS-aided NOMA network outperforms the IRS-aided OMA network under various target rate settings. The gap reduces when the target rate is very small since most resources are allocated to the user with better combined channel gain. IRS-assisted NOMA scheme is seen to be more robust against the target rate increase due to its ability of using the single resource block to serve multiple users. We can also see that TDMA scheme outperforms FDMA scheme as the IRS can be adjusted to maximise each user's combined-channel in the TDMA scheme under dynamic phase adjustment.

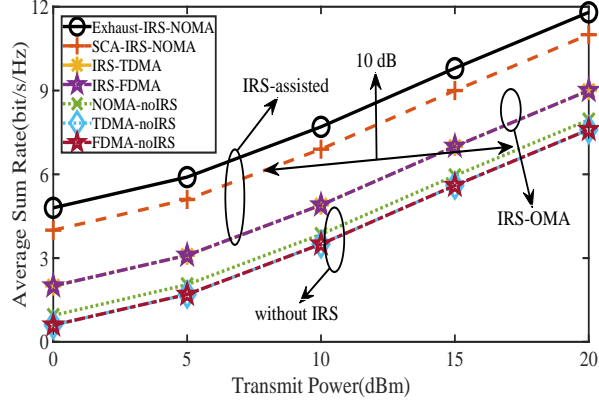


Fig. 7: The average sum rate versus power budget under one-time phase adjustment.

Average sum rate versus power budget under one-time phase adjustment: Fig.7 presents the proposed algorithms performances can obtain the close average sum rate to that obtained by the brutal search with lower complexity. The feasible solution in the discrete phase shifters adjustment that we achieve may experience performance losses for the quantization method. Applying IRS brings a 10 dB power consumption gain compared to the traditional NOMA scheme. The IRS-assisted NOMA scheme achieves higher average sum rate than traditional multiple access schemes while ensuring the system fairness. Moreover, in one-time adjustment scheme, the TDMA scheme has the same performance as the FDMA scheme as the reflecting elements can only be adjusted once at the nodes of fading blocks.

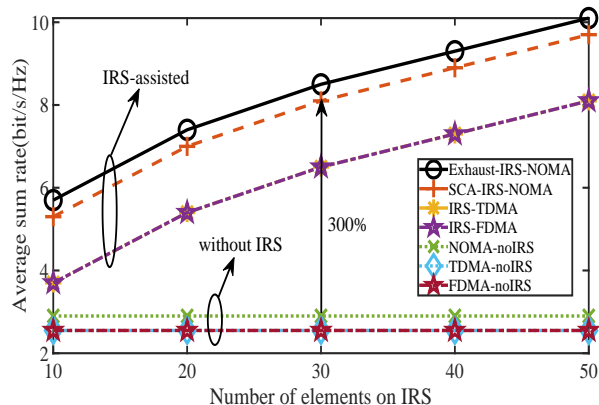


Fig. 8: The average sum rate versus number of IRS elements under one-time phase adjustment.

Average sum rate versus the number of IRS elements under one-time phase adjustment:

In Fig. 8, the comparison between system average data rate of various multiple access schemes versus the amount of reflecting elements N is presented. We can observe that IRS aided schemes outperforms the other schemes without IRS. Moreover, with the increase on phase elements N , the system performance is further enhanced. The larger number of reflecting elements gives flexibility on phase shifter adjustment and leads to higher combined channel gains. The received power level can be significantly increased with more reflecting elements, as more signals' power is reflected to served users.

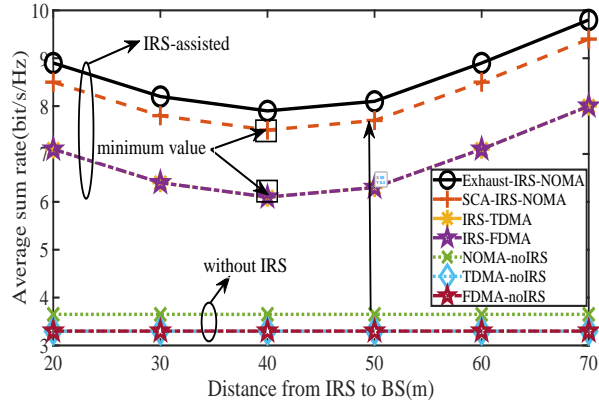


Fig. 9: The average sum rate versus distance from IRS to BS under one-time phase adjustment.

Average sum rate versus distance from IRS to BS under one-time phase adjustment: As shown in Fig. 9, the average rate performance of the IRS-assisted systems first decrease when the IRS is deployed close to the BS. After achieving the minimum average data rate, at a distance of 40m, the performance starts to increase. Observe that the concatenated channel response reaches the minimum data rate when the IRS is deployed in the middle BS and users. The average sum rate will be enhanced by a better IRS-aided link achieved from the shorter distance between the IRS and the user. Thus, carefully choosing the IRS location is very important for enhancing the system performance.

V. CONCLUSION

The IRS has been applied in downlink transmission with two users over fading channels for enhancing the average sum rate. Specifically, IRS assisted NOMA and OMA schemes were investigated. Additionally, we divided all fading states into several fading blocks and the phase

shifters were adjusted at the nodes of the fading blocks. For phase shift design, we proposed an effective solution using SCA to obtain high quality solutions. In addition, a SROCR method was applied to deal with the rank-one constraint. Then, we obtain locally optimal continuous phase shifters. The discrete phase shifters were obtained by a quantization scheme. For power allocation in each fading state, we solved the non-convex optimization problems using the dual decomposition method leveraging time-sharing conditions. Then, the average sum rate was maximized via the Lagrangian dual decomposition. Simulation results have revealed that in the downlink system over fading channels, the IRS assisted NOMA scheme can enhance the system performance significantly.

REFERENCES

- [1] L. Dai, B. Wang, Y. Yuan, S. Han, I. Chih-Lin, and Z. Wang, “Non-orthogonal multiple access for 5G: solutions, challenges, opportunities, and future research trends,” *IEEE Commun. Mag.*, vol. 53, no. 9, pp. 74–81, Sep. 2015.
- [2] S.-Y. Lien, S.-L. Shieh, Y. Huang, B. Su, Y.-L. Hsu, and H.-Y. Wei, “5G new radio: Waveform, frame structure, multiple access, and initial access,” *IEEE Commun. Mag.*, vol. 55, no. 6, pp. 64–71, Jun. 2017.
- [3] K. B. Letaief, W. Chen, Y. Shi, J. Zhang, and Y.-J. A. Zhang, “The roadmap to 6G: AI empowered wireless networks,” *IEEE Commun. Mag.*, vol. 57, no. 8, pp. 84–90, Aug. 2019.
- [4] X. Mu, Y. Liu, L. Guo, J. Lin, and N. Al-Dhahir, “Exploiting intelligent reflecting surfaces in multi-antenna aided NOMA systems,” *arXiv preprint arXiv:1910.13636*, 2019.
- [5] Y.-C. Liang, R. Long, Q. Zhang, J. Chen, H. V. Cheng, and H. Guo, “Large intelligent surface/antennas (LISA): Making reflective radios smart,” *arXiv preprint arXiv:1906.06578*, 2019.
- [6] S. Gong, X. Lu, D. T. Hoang, D. Niyato, L. Shu, D. I. Kim, and Y.-C. Liang, “Towards Smart Radio Environment for Wireless Communications via Intelligent Reflecting Surfaces: A Comprehensive Survey,” *arXiv preprint arXiv:1912.07794*, 2019.
- [7] M. Di Renzo, A. Zappone, M. Debbah, M.-S. Alouini, C. Yuen, J. de Rosny, and S. Tretyakov, “Smart Radio Environments Empowered by Reconfigurable Intelligent Surfaces: How it Works, State of Research, and Road Ahead,” *arXiv preprint arXiv:2004.09352*, 2020.
- [8] A. El Shafie, N. Al-Dhahir, Z. Ding, and R. Hamila, “On the Delay/Throughput-Security Tradeoff in Wiretap TDMA Networks With Buffered Nodes,” *IEEE Trans. Wireless Commun.*, vol. 18, no. 8, pp. 3948–3960, Jun. 2019.
- [9] M. Jung, W. Saad, Y. Jang, G. Kong, and S. Choi, “Performance analysis of large intelligent surfaces (LISs): Asymptotic data rate and channel hardening effects,” *IEEE Trans. Wireless Commun.*, vol. 19, no. 3, pp. 2052–2065, Jan. 2020.
- [10] W. Tang, M. Z. Chen, X. Chen, J. Y. Dai, Y. Han, M. Di Renzo, Y. Zeng, S. Jin, Q. Cheng, and T. J. Cui, “Wireless communications with reconfigurable intelligent surface: Path loss modeling and experimental measurement,” *arXiv preprint arXiv:1911.05326*, 2019.
- [11] S. Li, B. Duo, X. Yuan, Y.-C. Liang, and M. Di Renzo, “Reconfigurable intelligent surface assisted UAV communication: Joint trajectory design and passive beamforming,” *IEEE Wireless Commun. Lett.*, Jan. 2020.

- [12] Ö. Özdogan, E. Björnson, and E. G. Larsson, “Intelligent reflecting surfaces: Physics, propagation, and pathloss modeling,” *IEEE Wireless Commun. Lett.*, Dec. 2019.
- [13] C. Huang, A. Zappone, G. C. Alexandropoulos, M. Debbah, and C. Yuen, “Reconfigurable intelligent surfaces for energy efficiency in wireless communication,” *IEEE Trans. Wireless Commun.*, vol. 18, no. 8, pp. 4157–4170, Jun. 2019.
- [14] G. Yang, Y.-C. Liang, R. Zhang, and Y. Pei, “Modulation in the air: Backscatter communication over ambient OFDM carrier,” *IEEE Trans. Commun.*, vol. 66, no. 3, pp. 1219–1233, Nov. 2017.
- [15] Q. Zhang, H. Guo, Y.-C. Liang, and X. Yuan, “Constellation learning-based signal detection for ambient backscatter communication systems,” *IEEE J. Sel. Areas Commun.*, vol. 37, no. 2, pp. 452–463, Sep. 2018.
- [16] R. Long, H. Guo, L. Zhang, and Y.-C. Liang, “Full-duplex backscatter communications in symbiotic radio systems,” *IEEE Access*, vol. 7, pp. 21 597–21 608, Feb. 2019.
- [17] H. Guo, Y.-C. Liang, J. Chen, and E. G. Larsson, “Weighted sum-Rate maximization for reconfigurable intelligent surface aided wireless networks,” *IEEE Trans. Wireless Commun.*, Feb. 2020.
- [18] M. Jung, W. Saad, Y. Jang, G. Kong, and S. Choi, “Reliability analysis of large intelligent surfaces (LISs): Rate distribution and outage probability,” *IEEE Wireless Commun. Lett.*, vol. 8, no. 6, pp. 1662–1666, Aug. 2019.
- [19] S. Zhang and R. Zhang, “Capacity characterization for intelligent reflecting surface aided MIMO communication,” *arXiv preprint arXiv:1910.01573*, 2019.
- [20] H. M. Al-Obiedollah, K. Cumanan, J. Thiyyagalingam, A. G. Burr, Z. Ding, and O. A. Dobre, “Energy efficient beamforming design for MISO non-orthogonal multiple access systems,” *IEEE Trans. Commun.*, vol. 67, no. 6, pp. 4117–4131, Feb. 2019.
- [21] T. Hou, Y. Liu, Z. Song, X. Sun, and Y. Chen, “Multiple antenna aided NOMA in UAV networks: A stochastic geometry approach,” *IEEE Trans. Commun.*, vol. 67, no. 2, pp. 1031–1044, Oct. 2018.
- [22] Y. Liu, Z. Qin, M. Elkashlan, A. Nallanathan, and J. A. McCann, “Non-orthogonal multiple access in large-scale heterogeneous networks,” *IEEE J. Sel. Areas Commun.*, vol. 35, no. 12, pp. 2667–2680, Jul. 2017.
- [23] Y. Liu, Z. Qin, M. Elkashlan, Z. Ding, A. Nallanathan, and L. Hanzo, “Nonorthogonal multiple access for 5G and beyond,” *Proc. IEEE*, vol. 105, no. 12, pp. 2347–2381, Dec. 2017.
- [24] M. Shirvanimoghaddam, M. Dohler, and S. J. Johnson, “Massive non-orthogonal multiple access for cellular IoT: Potentials and limitations,” *IEEE Commun. Mag.*, vol. 55, no. 9, pp. 55–61, Sep. 2017.
- [25] Z. Ding, P. Fan, and H. V. Poor, “Impact of user pairing on 5G nonorthogonal multiple-access downlink transmissions,” *IEEE Trans. Veh. Technol.*, vol. 65, no. 8, pp. 6010–6023, Sep. 2015.
- [26] N. S. Perović, M. Di Renzo, and M. F. Flanagan, “Channel capacity optimization using reconfigurable intelligent surfaces in indoor mmWave environments,” *arXiv preprint arXiv:1910.14310*, 2019.
- [27] K. Ntontin, J. Song, and M. Di Renzo, “Multi-antenna relaying and reconfigurable intelligent surfaces: End-to-end SNR and achievable rate,” *arXiv preprint arXiv:1908.07967*, 2019.
- [28] E. Basar, “Transmission through large intelligent surfaces: A new frontier in wireless communications,” in *Proc. 2019 European Conference on Networks and Communications (EuCNC)*, Valencia, Spain, Jun. 2019, pp. 112117.
- [29] Q. Wu and R. Zhang, “Intelligent reflecting surface enhanced wireless network via joint active and passive beamforming,” *IEEE Trans. Wireless Commun.*, vol. 18, no. 11, pp. 5394–5409, Aug. 2019.
- [30] H. Han, J. Zhao, D. Niyato, M. Di Renzo, and Q.-V. Pham, “Intelligent reflecting surface aided network: Power control for physical-layer broadcasting,” *arXiv preprint arXiv:1910.14383*, 2019.

- [31] X. Guan, Q. Wu, and R. Zhang, "Intelligent reflecting surface assisted secrecy communication via joint beamforming and jamming," *arXiv preprint arXiv:1907.12839*, 2019.
- [32] Q.-U.-A. Nadeem, A. Kammoun, A. Chaaban, M. Debbah, and M.-S. Alouini, "Asymptotic max-min SINR analysis of reconfigurable intelligent surface assisted MISO systems," Apr. 2020.
- [33] G. Yang, X. Xu, and Y.-C. Liang, "Intelligent reflecting surface assisted non-orthogonal multiple access," *arXiv preprint arXiv:1907.03133*, 2019.
- [34] Y. Liu, Z. Qin, M. Elkashlan, Y. Gao, and L. Hanzo, "Enhancing the physical layer security of non-orthogonal multiple access in large-scale networks," *IEEE Trans. Wireless Commun.*, vol. 16, no. 3, pp. 1656–1672, Jan. 2017.
- [35] X. Mu, Y. Liu, L. Guo, J. Lin, and N. Al-Dhahir, "Capacity and optimal resource allocation for IRS-assisted multi-user communication systems," *arXiv preprint arXiv:2001.03913*, 2020.
- [36] T. Hou, Y. Liu, Z. Song, X. Sun, Y. Chen, L. Hanzo *et al.*, "Reconfigurable intelligent surface aided NOMA networks," *arXiv preprint arXiv:1912.10044*, 2019.
- [37] M. Fu, Y. Zhou, and Y. Shi, "Reconfigurable intelligent surface empowered downlink non-orthogonal multiple access," *arXiv preprint arXiv:1910.07361*, 2019.
- [38] X. Yue and Y. Liu, "Performance analysis of intelligent reflecting surface assisted NOMA networks," *arXiv preprint arXiv:2002.09907*, 2020.
- [39] Z. Ding and H. V. Poor, "A simple design of IRS-NOMA transmission," *arXiv preprint arXiv:1907.09918*, 2019.
- [40] H. Xing, Y. Liu, A. Nallanathan, Z. Ding, and H. V. Poor, "Optimal throughput fairness tradeoffs for downlink non-orthogonal multiple access over fading channels," *IEEE Trans. Wireless Commun.*, vol. 17, no. 6, pp. 3556–3571, Mar. 2018.
- [41] L. Li and A. J. Goldsmith, "Capacity and optimal resource allocation for fading broadcast channels. I. Ergodic capacity," *IEEE Trans. Inf. Theory*, vol. 47, no. 3, p. 10831102, Mar. 2001.
- [42] L. Li and A. J. Goldsmith, "Capacity and optimal resource allocation for fading broadcast channels. II. Outage capacity," *IEEE Trans. Inf. Theory*, vol. 47, no. 3, pp. 1103–1127, Mar. 2001.
- [43] V. Asghari and S. Aissa, "Resource management in spectrum-sharing cognitive radio broadcast channels: adaptive time and power allocation," *IEEE Trans. Commun.*, vol. 59, no. 5, pp. 1446–1457, Mar. 2011.
- [44] P. Cao, J. Thompson, and H. V. Poor, "A sequential constraint relaxation algorithm for rank-one constrained problems," in *Proc. European Signal Processing Conf (EUSIPCO)*, Aug. 2017, pp. 10601064.
- [45] W. Yu and R. Lui, "Dual methods for nonconvex spectrum optimization of multicarrier systems," *IEEE Trans. Commun.*, vol. 54, no. 7, pp. 1310–1322, Jul. 2006.
- [46] S. Boyd, S. P. Boyd, and L. Vandenberghe, *Convex optimization*. Cambridge university press, 2004.